


## Article

# Understanding the Influence of Biochar Augmentation in Anaerobic Digestion by Principal Component Analysis

Jessica Quintana-Najera <sup>1,2,\*</sup> , A. John Blacker <sup>2,3</sup>, Louise A. Fletcher <sup>4</sup> and Andrew B. Ross <sup>2,\*</sup><sup>1</sup> Faculty of Chemical and Biological Sciences, Autonomous University of Sinaloa, Culiacan 80010, Mexico<sup>2</sup> School of Chemical and Process Engineering, University of Leeds, Leeds LS2 9JT, UK<sup>3</sup> Institute of Process Research and Development, School of Chemistry, University of Leeds, Leeds LS2 9JT, UK<sup>4</sup> School of Civil Engineering, University of Leeds, Leeds LS2 9JT, UK

\* Correspondence: j.quintana@uas.edu.mx (J.Q.-N.); a.b.ross@leeds.ac.uk (A.B.R.)

**Abstract:** Biochar addition in anaerobic digestion has been repeatedly reported to improve methane production, however, this ability is not well understood. This work aims to understand and correlate the most important factors influencing anaerobic digestion performance using principal component analysis along with quantitative and qualitative descriptive analysis to evaluate the variations of methane production with the addition of biochar. Reports from the literature using biochar produced from several feedstocks under variable pyrolysis conditions and therefore different compositions were carefully gathered and compared with their own non-biochar controls. Woody-derived biochars, produced at 450–550 °C, containing an ash content of 3.1–6.3%, and an O:C ratio of 0.20, were responsible for having the greatest positive effect. The amount of biochar added to the digesters also influences anaerobic digestion performance. Increasing biochar loads favours the production rate, although this can be detrimental to methane yields, thereby, biochar loads of approximately 0.4–0.6% (*w/v*) appear to be optimal. This work provides a guide for those interested in biochar augmentation in anaerobic digestion and identifies the main interactions between the variables involved.

**Keywords:** biochar; anaerobic digestion; pyrolysis; principal component analysis



**Citation:** Quintana-Najera, J.; Blacker, A.J.; Fletcher, L.A.; Ross, A.B.

Understanding the Influence of Biochar Augmentation in Anaerobic Digestion by Principal Component Analysis. *Energies* **2023**, *16*, 2523. <https://doi.org/10.3390/en16062523>

Academic Editor: Attilio Converti

Received: 21 February 2023

Revised: 3 March 2023

Accepted: 5 March 2023

Published: 7 March 2023



**Copyright:** © 2023 by the authors. Licensee MDPI, Basel, Switzerland. This article is an open access article distributed under the terms and conditions of the Creative Commons Attribution (CC BY) license (<https://creativecommons.org/licenses/by/4.0/>).

## 1. Introduction

The role of biochar (BC) in amending the stressful factors affecting the performance of anaerobic digestion (AD) has been highly reported but is not well understood. Among the general accounts, it has been stated that BC can couple the biological and chemical transformations occurring during AD, resulting in better performance and stability [1]. It is generally accepted that BC supports the immobilisation of cells from anaerobic sludge; provides a buffering effect; adsorbs metabolites; reduces ammonia inhibition; and acts as an intermediary during the direct interspecies electron transfer (DIET) process [2].

Wu et al. [2] proposed a mechanism for explaining the complexity of how BC facilitates methane generation. The H<sub>2</sub> produced during acidogenesis increases the partial pressure of the system, thus the rapid use of H<sub>2</sub> and subsequent production of methane is key. This requires transferring electrons between fermentative bacteria and methanogens through the electron carriers H<sub>2</sub> or formate via the hydrogenases and formate dehydrogenases (FDH) enzymes. DIET interactions are a mechanism involving bioelectric connections via biological compounds, such as conductive pili (e-pili), c-type cytochrome (OmcS) and electron transport proteins. It is necessary for the microorganisms involved in DIET to have intimate direct contact with the electron transport proteins on the outer membrane to deliver the electrical contact. Remarkably, microorganisms can also exhibit DIET via exogenous non-biological conductive materials that emulate the function of pili or OmcS, such as biochar [2].

The surface functionality of the BCs, particularly oxygenated functional groups (OFGs), such as C-O, C=O, OH and COOH, are the predominant and most important features of

surface chemistry, and responsible for most of their interaction with organic matter [3]. The pyrolysis temperature (PT) is the main factor determining the number of OFGs on the BCs. The OFGs within the redox-active structures, quinone-hydroquinone moieties and/or conjugated  $\pi$ -electron systems of the BCs aromatic sub-structures facilitate the DIET interactions [4]. Accordingly, the BCs enable the transfer of electrons from bulk chemical electron donors to a receiving organic compound between  $H_2$ -producing bacteria and  $H_2$ -consuming methanogens, thus enhancing reaction rates and kinetic efficiencies [5,6]. The OFGs serve as anchoring sites for intermolecular and interspecies interactions [7,8]. There have been repeated reports regarding the benefits of adding BCs with a large presence of OFGs to improving AD performance [6,9,10].

The ability of BC to amend ammonia inhibition has also been attributed to the cation exchange capacity (CEC), and the H-bonds between the ammonium ions and the functional groups of the BC [11,12]. As previously stated, the potential of BC to act as a buffering agent has been attributed principally to the organic functional groups, including OFGs and/or conjugated  $\pi$ -electron systems [6]; and to a lesser extent to the ash-inorganic alkalis, and organic alkalis confined in the BC [13]. The BC also promotes the growth of archaea (*Methanosaeta* and *Methanosarcina*) and bacteria (*Bacteroidetes* and *Geobacter*) involved in volatile fatty acid (VFA) degradation and methane production [7,14–16]. Regardless of the efforts for elucidating the mechanisms involved during BC addition in AD, the practical application for engineering purposes still requires an understanding of how to proceed.

The addition of BC in batch laboratory scale systems reported in the literature has resulted in diverse and often ambiguous effects on methane production. This could be due to a series of factors, such as the pyrolysis conditions defining the properties of the BC [11], the anaerobic digestion conditions [17], the inoculation [18], and the amount of biochar added to the digester [19,20]. Previous studies have investigated a wide variety of BC and most authors have attempted to attribute their effect on AD to the physicochemical properties of the BC. Numerous reviews have gathered information from publications and attempted to explain how BC influences AD performance [11,21–23]. However, the statistical analysis of large datasets for correlating the inherent properties of the BCs and their effective influence on AD performance has not been attempted.

To achieve this, principal component analysis (PCA) could be a valuable approach to create an understanding and even set the standards for BC augmentation on AD. PCA could determine which variables explain most of the variance in a dataset and how they are correlated, identifying those highly influential for BC augmentation and how they interact together. There is only one recent report evaluating the effect of BCs from rice husk (RH), sewage sludge (SS) and softwood (SW) produced at 550 °C and activated by  $CO_2$  while employing PCA for elucidating this relationship [24]. They processed 11 factors to identify correlations, including surface area (SA), pore volume (PV), pore size, pH, electrical conductivity (EC), ash, volatile matter (VM), fixed and total carbon (FC and TC, respectively), H:C and O:C ratios, biogas and methane ( $CH_4$ ) productions. They observed a large correlation between  $CH_4$ , O:C, H:C, and VM, while the unrelated  $CH_4$  and biogas were attributed to the removal of  $CO_2$  by BC through adsorption and mineralization or the increased conversion of  $CO_2$  to  $CH_4$  mediated by BC. The influence on biogas generation was correlated to PV, SA, FC and TC, and negatively correlated to ash. It is worth mentioning that PCA is intended for the analysis of a large dataset and in this case, they use only their experimental data by testing three BCs, three activated BCs, one substrate (mixed wastewater sludge), and one set of AD conditions.

The interaction and response to changes taking place in complex systems, such as AD, are difficult to understand and can even lead to ambiguous observations. Hence, it is important to evaluate the factors both individually and collectively to understand and correlate the behaviours observed. To the best of our knowledge, this is the first work evaluating a large dataset for the augmentation of biochar during anaerobic digestion and employing PCA for this purpose. Therefore, this work aims to understand and correlate the most important factors influencing AD performance using the multivariate statistical

method PCA, along with quantitative and qualitative descriptive analysis, to evaluate the variations of AD performance with the addition of BCs. Moreover, investigating additional factors that can also contribute to methane production, including choice of substrate and composition, ISR and BC load.

## 2. Materials and Methods

### 2.1. Selection of Data

Reports of biochar augmentation in AD at mesophilic conditions were compiled in Tables 1–4. The criteria for selecting the reports included mesophilic conditions (35–37 °C), the use of batch digesters and that each publication provided enough information about the origin and composition of the BCs, digestion conditions and the effect of the BC on AD to allow the analysis. Information about the BCs included feedstock, pyrolysis temperature, O:C ratio and ash content, the importance of these parameters is based on their reported impact on BC augmentation in AD [6,11]. Most BCs derived from a lignocellulosic woody source, other feedstocks included high-cellulose (water hyacinth, switchgrass, and bamboo), algae (*F. serratus*) and high-protein feedstock (dairy manure and canola meal), produced at variable pyrolysis conditions (350–900 °C). Information about the pyrolysis conditions employed is listed in the tables as provided by each publication, although many failed to state a detailed description. For AD conditions, the systems consisted of batch experiments using either an Automatic Methane Potential Test System (AMPTS II) (Bio-process Control, Sweden) or serum bottles of variable sizes (100–1100 mL). The reports also included the choice of substrate, amount of substrate, biochar load (BCL), and inoculum-to-substrate ratio (ISR). For the effect of BC in AD, the selected data must include a control without BC addition to be able to compare the effect of BC on the most significant performance parameters.

### 2.2. Biochar Effect on Anaerobic Digestion

To establish the effect of BC addition on AD performance for the set of conditions for each publication gathered in Tables 1–4, the AD parameters corresponded to those obtained at the end of the fermentation and once the stationary phase was achieved. The changes in the kinetic parameters were calculated in comparison to their corresponding non-BC control as follows:

$$\text{BMP (\%)} = \frac{(\text{BMP}_{\text{BC}} - \text{BMP}_{\text{C}}) * 100}{\text{BMP}_{\text{C}}} \quad (1)$$

$$\mu_{\text{m}} (\%) = \frac{(\mu_{\text{m,BC}} - \mu_{\text{m,C}}) * 100}{\mu_{\text{m,C}}} \quad (2)$$

$$\lambda \text{ reduction (\%)} = \frac{(\lambda_{\text{BC}} - \lambda_{\text{C}}) * 100}{\lambda_{\text{C}}} \quad (3)$$

where the biochemical methane potential (BMP) corresponds to the maximum and final methane yield (mL CH<sub>4</sub>/g VS);  $\mu_{\text{m}}$  to the maximum methane production rate (mL CH<sub>4</sub>/g VS-day); and  $\lambda$  to the lag phase (days); the parameters are expressed on the mentioned units unless stated otherwise. The denotation BC and C correspond to systems supplemented with biochar and the non-biochar control, respectively.

**Table 1.** Summary of the reports for the biochar addition on anaerobic digestion of model carbohydrate substrates.

Biochar Feedstock	Pyrolysis Conditions	BC Load (% w/v)	AD Conditions	ISR	BMP	$\mu_m$	$\lambda$ (Days)	Ref.
Oak wood	Commercial SP mono retort reactor	0			265.9	11.8	0	
	450 °C	3			285.5	28.1	1.5	
	650 °C	3			251.6	13.1	13.1	
Fucus serratus	SP fixed bed, N <sub>2</sub> flow, HR 5 °C/min		AMPTS, 37 °C, HRT 30 d, cellulose 5 g VS/L	1				[10]
	450 °C, 1 h	3			38.3	4.9	17.3	
	600 °C, 1 h	3			41.1	1.9	3.6	
Water hyacinth	450 °C, 1 h	3			294.2	27.3	1.2	
	600 °C, 1 h	3			266.0	12.3	3.3	
Rice straw	Hypoxic conditions, PS < 1 mm	0	AMPTS, 35 °C, HRT 25 d, glucose 9 g/L	0.18	142.0	6.5		
Corn stover		0.5			143.6	8.2		
Bamboo		0.5			138.0	6.3		
Pine wood		0.5			145.0	9.8	NR	[25]
Oak wood		0.5			156.4	9.7		
Apple wood		0.5			158.9	9.0		
					163.8	9.2		
Fruitwoods	800–900 °C PS 0.5–1 mm	0	Serum bottle, 35 °C, HRT 120 d, glucose 6 g/L TAN 0.3 g/L		13.2 <sup>a</sup>	1.3 <sup>b</sup>	23.5	
		1			12.9 <sup>a</sup>	1.5 <sup>b</sup>	16.3	
	800–900 °C PS 0.5–1 mm	0	Glucose 6 g/L, TAN 3.5 g-N/L	0.17	13.5 <sup>a</sup>	0.59 <sup>b</sup>	30.5	
		1			13.3 <sup>a</sup>	0.65 <sup>b</sup>	26.5	[12]
	800–900 °C PS 0.5–1 mm	0	Glucose 6 g/L, TAN 7 g-N/L		13.6 <sup>a</sup>	0.34 <sup>b</sup>	63.5	
		1			13.8 <sup>a</sup>	0.42 <sup>b</sup>	48.4	
	PS 2–5 mm	1		15.2 <sup>a</sup>	0.50 <sup>b</sup>	48.3		
	PS 75–150 $\mu$ m	1		14.0 <sup>a</sup>	0.49 <sup>b</sup>	59.8		
Fruitwoods		0	Serum bottle, HRT 22 d, glucose 2 g/L	0.5	15.7 <sup>a</sup>	2.8 <sup>b</sup>	12.7	
		1			15.3 <sup>a</sup>	2.3 <sup>b</sup>	10.6	
		0	HRT 32 d, glucose 4 g/L	0.25	16.6 <sup>a</sup>	1.1 <sup>b</sup>	15.8	
		1			13.7 <sup>a</sup>	2.1 <sup>b</sup>	14.0	
		0	HRT 38 d, glucose 6 g/L	0.17	14.2 <sup>a</sup>	1.3 <sup>b</sup>	23.4	
		1			13.7 <sup>a</sup>	1.5 <sup>b</sup>	16.3	[26]
		0	HRT 42 d, glucose 8 g/L	0.125	15.1 <sup>a</sup>	1.0 <sup>b</sup>	25.0	
		1			13.3 <sup>a</sup>	1.0 <sup>b</sup>	19.6	

PS particle size; SP slow pyrolyser; HR heating rate; BMP expressed in mL CH<sub>4</sub>/g and  $\mu_m$  expressed in mL CH<sub>4</sub>/g·d, unless stated otherwise; <sup>a</sup>—BMP (mmol CH<sub>4</sub>/g); <sup>b</sup>— $\mu_m$  (mmol CH<sub>4</sub>/g·d); HRT hydraulic retention time; TAN total ammonia nitrogen; NR not reported.

The values calculated as described in Equations (1)–(3) are shown in Abbreviation part. These effects were expressed as % of variation where 0% represents the value obtained as the same as the control; thus, the addition of BC offered no effect on that parameter. Conversely, 100% states that the BC addition doubled the value obtained by the control. Moreover, a positive value indicates an improvement of that parameter, while a negative value states a detrimental effect due to BC addition.

**Table 2.** Summary of the reports for the biochar addition on anaerobic digestion of food waste and organic fraction of the municipal solid waste (OFMSW).

Feedstock	Pyrolysis Conditions	BC Load (% w/v)	AD Conditions	ISR	BMP	$\mu_m$	$\lambda$ (Days)	Ref.	
Pine sawdust	Indirectly fired kiln, size PS 12–25.9 $\mu\text{m}$ 650 °C, 20 m	0	Serum bottle 100 mL, HRT 40 d, 37 °C, food waste 496 g VS/L		1487 <sup>a</sup>	272 <sup>b</sup>	6	[27]	
		1.5			2092 <sup>a</sup>	362 <sup>b</sup>	6		
	1.5	2187 <sup>a</sup>			389 <sup>b</sup>	6			
Vineyard pruning	Pilot plant semi-continuous electrical reactor, anoxic, no inert gas, 550 °C, 15 min	0	Erlenmeyer flask 250 mL, HRT 54 d, 37 °C, citrus peel waste	1	103	10.9	16.8	[28]	
		1			209	14.3	9.8		
		3			298	14.2	9.3		
Walnut shell	Commercial downdraft gasifier 900 °C	0 0.35 0.70	Serum bottle 650 mL, HRT 55 d, 37 °C, food waste 4 g VS/L	1.36	484 492 131	NR	NR	[19]	
Rice straw	Furnace, N <sub>2</sub> flow 500 °C, 2 h	0 0.5	AMPTS, HRT 25 d, 35 °C, OFMSW 8.6 g/L	1	174.2 <sup>c</sup> 92.4 <sup>c</sup>	72.5 <sup>d</sup> 40.1 <sup>d</sup>	1.8 1.1	[16]	
Fruitwoods	Commercial kiln 800–900 °C PS <1 mm	0	Serum bottle 1100 mL, 210 d, 35 °C, food waste 4 g/L	2	490.0	0.05	55.4	[29]	
		0.2			480.1	0.08	65.8		
		0.5			493.1	0.07	51.6		
		1			507.5	0.15	49		
		0			440.0	0.03	89.9		
	Commercial kiln 800–900 °C PS <1 mm	0.2	Food waste 8 g/L	1	460.3	0.07	51		
		0.5			530.5	0.06	50.5		
		1			476.6	0.07	41.1		
		0			Food waste 10 g/L	0.8	340.0	0.03	123.9
		0.2					490.2	0.04	79
0.5	478.1	0.06	57						
1	471.9	0.05	68.1						
Pine sawdust	Indirectly fired kiln 650 °C, 20 min PS 3.6–25.9 $\mu\text{m}$	0	Serum bottle 100 mL, HRT 40 d, 35 °C, food waste 13.7 g/L		1070 <sup>a</sup>	113 <sup>b</sup>	10	[20]	
		0.83			1137 <sup>a</sup>	156 <sup>b</sup>	5.9		
		1.66			1057 <sup>a</sup>	160 <sup>b</sup>	5.7		
		2.51			956 <sup>a</sup>	145 <sup>b</sup>	5.5		
		3.33			931 <sup>a</sup>	138 <sup>b</sup>	5.7		
Coconut shell Wood Rice husk	Commercial 450 °C PS 1.7–2.0 mm	0	Serum bottle 500 mL, HRT 30 d, 35 °C, citrus peel waste	0.3	165.9	21.8	13.4	[30]	
		0.96			186.8	26.0	7.3		
		0.96			171.3	18.4	6.8		
		0.96			172.1	26.6	12.8		

PS particle size; BMP expressed in mL CH<sub>4</sub>/g and  $\mu_m$  expressed in mL CH<sub>4</sub>/g·d, unless stated otherwise; <sup>a</sup>—BMP (mL CH<sub>4</sub>/L); <sup>b</sup>— $\mu_m$  (mL CH<sub>4</sub>/L·d); <sup>c</sup>—BMP (mL CH<sub>4</sub>); <sup>d</sup>— $\mu_m$  (mL CH<sub>4</sub>/d); HRT hydraulic retention time; NR not reported.

**Table 3.** Summary of the reports for the biochar addition on anaerobic digestion of sewage sludge, animal manure, bio-oil aqueous phase (BOAP) and aqueous pyrolysis liquid (APL).

Feedstock	Pyrolysis Conditions	BC Load (% w/v)	Substrate	ISR	BMP	$\mu_m$	$\lambda$ (Days)	Ref.
Vineyard pruning	Pilot plant semi-continuous electrical reactor, anoxic, no inert gas, 550 °C, 15 min	0	Erlenmeyer flask 250 mL, HRT 54 d, 37 °C, sludge	1	273	18.7	7.9	[28]
		1			364	23.1	5.2	
		3			425	33.4	5.9	
Almond shell residue	Commercial semi-continuous electrically heated, anoxic 550 °C, 15 min	0	Serum bottle 250 mL, HRT 40 d, 35 °C, swine manure 6 g VS/L	1	298.7	21.2	9.2	[31]
		1.2			395.4	24.5	6.1	
		0	Pre-treated swine manure	1	416.7	27.5	5.9	
1.2	433.2	28.8			5.8			
Dairy manure	Muffle furnace HR 10 °C/min 350 °C, 3 h Size 420–600 $\mu$ m	0	Serum bottle 280 mL, 35 °C, HRT 35 d, dairy manure	NR	374.7	28.2	2.1	[32]
		0.1			394.9	29.9	1.9	
		1.0			466.5	37.4	1.5	
Ashe juniper	Semi-pilot Auger reactor, N <sub>2</sub> flow 400 °C, 30 min 600 °C, 30 min	0	Serum bottle 160 mL, 37 °C, HRT 10 d, BOAP 4 g COD/L	0.24	24	NR	NR	[9]
		1			296			
		1			88			
Canola meal	700 °C, 2 h 900 °C, 2 h	1			43	NR	NR	
		1			37			
Pine wood Oak wood	Commercial pilot-scale fluidised bed gasifier, gas recirculation and N <sub>2</sub> flow	0	2-step 600 mL digesters: (i) 37 °C/HRT 1.2 d; (ii) 53 °C/HRT 12 d, sludge	NR	0.31 <sup>a</sup>	72.5 <sup>b</sup>	NR	[33]
		3.1			0.31 <sup>a</sup>	82.9 <sup>b</sup>		
		6.3			0.31 <sup>a</sup>	71.4 <sup>b</sup>		
Oak wood	710 °C, 0.8 sec	2.8		NR	0.33 <sup>a</sup>	83.2 <sup>b</sup>	NR	
		5.6			0.32 <sup>a</sup>	79.4 <sup>b</sup>		
Cornstalk	Commercial pilot-scale fluidised bed gasifier, gas recirculation and N <sub>2</sub> flow 710 °C, 0.8 sec	0	Serum bottle 600 mL, HRT 25 d, 35 °C, sludge 4.3 g TS/L	2	488.9	125.5 <sup>b</sup>	NR	[34]
		0.8			494.3	160.1 <sup>b</sup>		
		1.1			494.9	144.5 <sup>b</sup>		
		1.3			495.2	143.6 <sup>b</sup>		
		1.6			494.5	131.5 <sup>b</sup>		
Cornstalk pellet	Fixed bed reactor, HR 100 °C/min, N <sub>2</sub> flow 400 °C, 10 min	0	Syringe 100 mL, HRT 225 d, 40°, APL 35 g COD/L	0.6	12 <sup>c</sup> 20 <sup>c</sup>	0.1 <sup>d</sup> 0.2 <sup>d</sup>	NR	[35]

HR heating rate; BMP expressed in mL CH<sub>4</sub>/g and  $\mu_m$  expressed in mL CH<sub>4</sub>/g·d, unless stated otherwise; <sup>a</sup>—BMP (mL CH<sub>4</sub>/g COD); <sup>b</sup>—BMP (mL CH<sub>4</sub>/d); <sup>c</sup>—BMP (g COD<sub>CH4</sub>/L); <sup>d</sup>— $\mu_m$  (g COD<sub>CH4</sub>/L·d); HRT hydraulic retention time; NR not reported.

**Table 4.** Summary of the reports for the biochar addition on anaerobic digestion of aquatic plants, algae, ammonium carbonate and anaerobic co-digestion of multiple substrates.

Feedstock	Pyrolysis Conditions	BC Load (% w/v)	Substrate	ISR	BMP	$\mu_m$	$\lambda$ (Days)	Ref.
Oak wood	Commercial SP mono retort reactor 450 °C	0	AMPTS, 37 °C, HRT 30 d, water hyacinth 5 g VS/L Samples from different sources	1	208.9	15.0	0.0	[36]
		0.5			217.7	24.9	1.5	
		1			141.7	13.0	0.4	
		0			201.3	20.2	0.0	
		0.5			163.3	15.8	0.0	
		1			196.6	17.5	0.0	
		0			177.1	19.8	0.0	
		0.5			141.4	32.6	0.2	
		0			91.6	6.8	0.0	
		0.5			53.7	5.0	0.0	
Oak wood	Commercial SP mono retort reactor 450 °C	0	AMPTS, 37 °C, HRT 30 d, <i>C. vulgaris</i> cellulose, 5 g VS/L, C/N 10	0.5	50.8	23.6	0.4	[37]
		3			232.7	9.5	1.0	
		0	C/N 20	0.8	91.2	39.5	1.0	
		3			239.1	10.0	0.0	
		0	C/N 30	0.9	136.2	22.7	0.5	
		3			241.2	12.4	0.0	
Waste wood	Commercial continuous rotatory kiln 700 °C, 1 h PS 75–500 $\mu\text{m}$	0	AMPTS, HRT 30 d, 37 °C, <i>L. digitata</i> 5 g VS/L	2	200.1	22.1	1.5	[38]
		0.03			211.5	25.8	0.8	
		0.06			212.9	24.2	0.8	
		0.12			234.0	24.7	0.7	
		0.5			180.0	19.5	1.3	
		1			179.7	20.3	1.4	
Sawdust	Muffle furnace, HR 10 °C/min, anoxic 500 °C, 1.5 h PS 0.25–1.0 mm	0	Serum bottle working volume 90 mL, 35 °C, HRT 55 d, food waste and sludge 2 g VS/L	0.67	111.7 <sup>a</sup>	6.7 <sup>b</sup>	21.2	[13]
		0.2			114.6 <sup>a</sup>	8.7 <sup>b</sup>	15.3	
		0.6			116.2 <sup>a</sup>	9.4 <sup>b</sup>	12.1	
		1.0			112.1 <sup>a</sup>	8.2 <sup>b</sup>	10.2	
		1.5			109.5 <sup>a</sup>	7.8 <sup>b</sup>	7.8	
		0			Erlenmeyer flask 250 mL, HRT 54 d, 37 °C, citrus peel waste and sludge	1	298	
1	500	66.3	3.6					
3	704	75.5	3.3					
Paper sludge-wheat husk	Commercial screw pyrolyser, no inert gas. Post-outgassed and quenched with water 500 °C, 20 min	0	Syringe 100 mL, HRT 63 d, 40 °C, (NH <sub>4</sub> ) <sub>2</sub> CO <sub>3</sub> TAN 0.5–5 g/kg	NR	4.4 <sup>c</sup>	0.03 <sup>d</sup>	NR	[39]
		2			4.5 <sup>c</sup>	0.03 <sup>d</sup>		

HR heating rate; PS particle size; BMP expressed in mL CH<sub>4</sub>/g and  $\mu_m$  in mL CH<sub>4</sub>/g·d, unless stated otherwise; <sup>a</sup>—BMP (mL CH<sub>4</sub>); <sup>b</sup>— $\mu_m$  (mL CH<sub>4</sub>/d); <sup>c</sup>—BMP (mL CH<sub>4</sub>/g); <sup>d</sup>— $\mu_m$  (d<sup>-1</sup>); NR not reported.

### 2.3. Principal Component Analysis

PCA is also known as a projection method, whose principal objective is the explanation of large data into smaller and more informative components. For this PCA analysis, eight variables to study were selected and divided into three categories: (i) related to the generation and properties of the BCs: pyrolysis temperature (PT), ash content, and O:C ratio; (ii) related to the AD conditions: inoculum-to-substrate ratio (ISR) and biochar load (BCL); (iii) related to the AD performance: effect of BC addition on BMP,  $\mu_m$  and  $\lambda$ . It is recommended to re-scale and homogenise the data when different scales and units are being used; in this case, the initial data used units of pH, °C, and percentage. To have a dataset suitable for PCA, the values for the variables calculated with Equations (1)–(3) and listed in Supplementary Table S1 were homogenised by transforming into mean-centred values and divided by their standard deviations according to Equation (4) [40]. The re-scaled dataset based on the difference between the control and standardised as described



are listed in Supplementary Table S2. The effect of BC addition on these variables are used for the PCA and the descriptive statistics.

$$\text{Standardised data} = \frac{\text{Mean centred value}}{\text{Standard deviation}} \quad (4)$$

The Kaiser–Meyer–Olkin (KMO) method, Bartlett’s test of sphericity and communalities were used to establish the adequacy of the PCA analysis. KMO examines the suitability of the data and is found between 0 and 1, where average values  $> 0.5$  are good and  $>0.9$  are near perfection. The communalities indicate the relationship or amount of common variance of each variable with the entire dataset. It is not desirable for the correlations to be extremely low or non-existent or to be extremely high because these might indicate a lack of variation in the data. Bartlett’s test of sphericity indicates if there is a significant difference among the correlations between the variables ( $p < 0.05$ ) [41]. Oblique rotation was used for the PCA analysis assuming that all factors could be correlated. The principal components (PCs) represent the most important sources of variability and explain a certain amount of information within the original data. The first PC contains the greatest source of information explaining the data set, whereas each subsequent PC contains less information than the previous one. PCs with eigenvalues greater than one are considered important and were thus retained [40]. The software SPSS Statistics 26 (IBM, New York, NY, USA) was used for the PCA analysis and Origin 2019 for the PCA plots.

#### Visual Representation of the Principal Component Analysis

The PCA biplot represents the data as scores and loadings. Scores correspond to each sample distributed in the space of the PCs describing the variability of the dataset. The distance of the samples distributed along the axis is an indication of how much of their information is contained within the PCs. Samples positively correlated are in a similar direction, while opposite directions indicate a negative correlation [42]. PCA loadings indicate the contribution placed on each variable to describe the PCs. Loadings with the highest values and located farther away from the origin indicate the most important variables, whereas those with values of approximately zero or closer to the origin contribute little to describing the samples in the PCs [40].

#### 2.4. Descriptive Analysis

The effect of BC addition over the response variables BMP,  $\mu_m$  and  $\lambda$  calculated as described in Equations (1)–(3) were correlated to the working variables used in each literature report, including PT, ash content, O:C ratio, ISR, and BC load. Box plots displayed the distribution of the large dataset through their quartiles. Individual comparisons of the effect of the working variables over the response variables were evaluated by analysis of variance at a confidence level of  $p < 0.05$ . All analyses were performed using the SPSS Statistics 26 software.

### 3. Results and Discussion

#### 3.1. Principal Component Analysis

The PCA exhibited average sample adequacy with a KMO value of 0.6 and a significant correlation between the variables according to Bartlett’s test of sphericity ( $p < 0.05$ ). The communalities were adequate within a range of 0.555 to 0.700 (Figure 1a); this suggests an appropriate amount of common variance for each variable with the entire dataset. Three PCs exhibiting Eigenvalues above 1 were maintained, describing 65.3% of the total variation in the dataset as shown in the scree plot (Figure 1b).



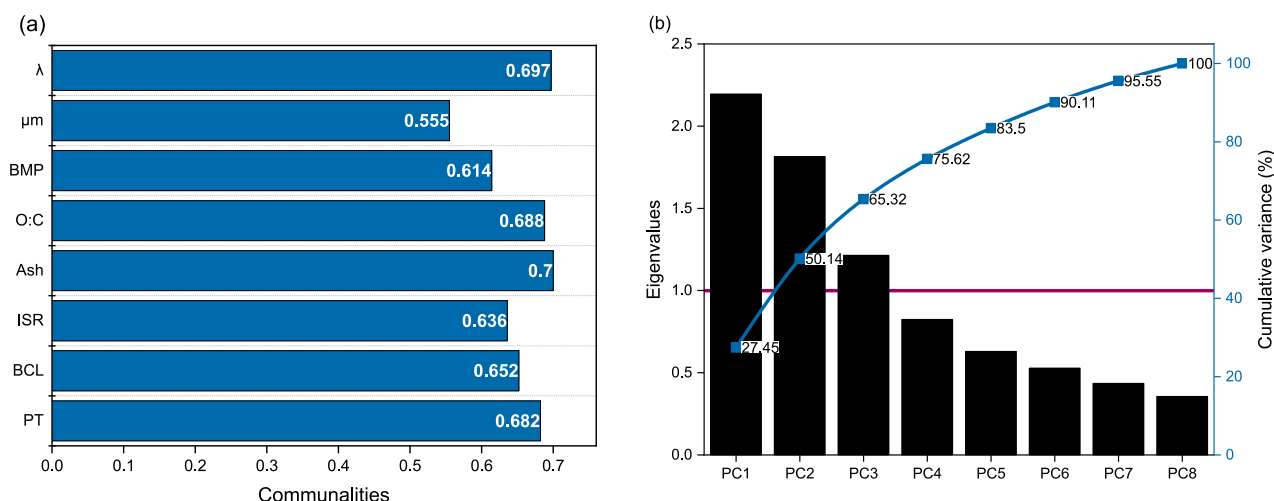


**Figure 1.** Results of the principal component analysis (PCA): (a) Communalities for the variance of each variable explained by the PCA; (b) Scree plot of the principal components (PCs) outlining the Eigenvalues and variance of the dataset. The PCs are the linear depiction of the original dataset and the total variance of the eight variables.

The PCs were visualised by two PCs at the time, with the biplot for PC1-PC2 and PC1-PC3 describing 50.11% and 42% of the dataset variation, respectively (Figure 2). Most scores were projected as scattered data lying along the PC1 indicating a higher influence by variables highly represented by PC1. The scores located in the space between the PC1-PC2 and PC1-PC3 axes are influenced by variables that are important on both PCs. In the biplot PC1-PC2 (Figure 2a), the loadings for BMP and O:C ratio were close to the origin, suggesting the least variability and contribution. For the biplot PC1-PC3 (Figure 2b), the variables PT, BCL, and  $\lambda$  were once more highly described by the PC1. The magnitude and distribution of the loadings on the PC area indicate that the variable BMP, O:C ratio and ISR yield were highly described by the PC3.

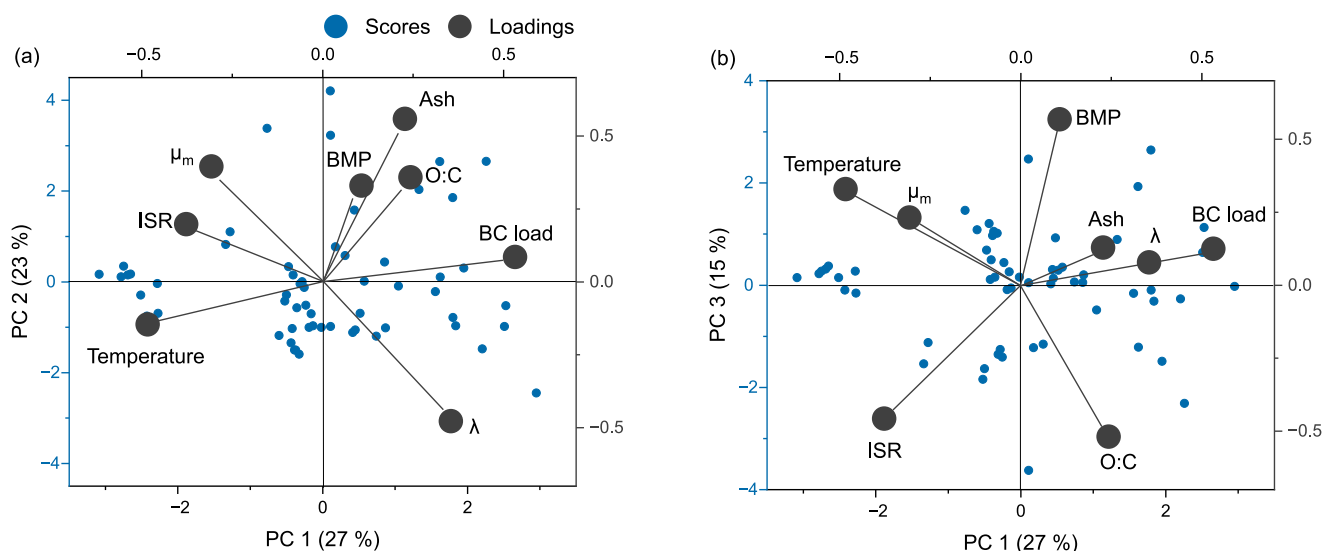


**Figure 2.** Principal component analysis biplot for the parameters influencing biochar augmentation in anaerobic digestion: (a) PC1 vs. PC2; (b) PC1 vs. PC3. Pyrolysis temperature (PT); methane yield (BMP);  $\mu_m$  methane production rate;  $\lambda$  lag phase; ISR inoculum-to-substrate ratio; biochar ash content; biochar O:C ratio dry ash-free basis; biochar load. The dataset is listed in Supplementary Table S2.

The angle between two vector loadings indicates their correlations, thus, the proximity leads to a higher correlation [42]. PT was moderately correlated to ISR and to a lesser

extent to  $\mu_m$ . The variables ash, O:C ratio and BMP were highly correlated, meaning that as the ash and O:C ratio of the BC increases, so does the methane yield (Figure 2a). The correlation between ash and O:C ratio was expected because both variables are related to the BC composition. These variables were orthogonal to PT, suggesting that increasing the pyrolysis temperature reduces the O:C ratio of the BCs, while the addition of higher temperature BCs to AD would reduce the positive effect on the BMP.

The angles separating the BMP and  $\mu_m$  were below  $90^\circ$ , suggesting a positive correlation; thereby, as the BMP increased so did the  $\mu_m$  (Figure 2a). The same principle applies to  $\mu_m$  and ISR; consequently, higher  $\mu_m$  could be achieved by employing larger ISRs, in agreement with the asserted role of inoculation on the initial activity and performance of the digester [18]. On the other hand, loadings orthogonal (perpendicular) to each other were negatively correlated as observed for ISR with BCL and  $\lambda$ . The correlation between  $\mu_m$  and  $\lambda$  was expected because of their time dependence. An orthogonal projection was also observed for the PT and BCL, meaning that as the carbonisation degree of the BC increases, its addition to the digester must be reduced. Moreover, BCL was independently correlated to the O:C ratio and  $\lambda$ . The BCL could be quantitatively correlated to the amount of BC and therefore the number of OFGs present in the digestate and responsible for facilitating the DIET process.

Figure 2b also suggests a correlation between the variable PT and  $\mu_m$ . The loading for  $\lambda$  is now near the ash and BCL variables, which could be attributed to the role of the BC in facilitating DIET interactions that promote the methanogenesis and reduce the  $\lambda$ . The position of the variables BMP and ISR largely described the PC3 and suggested that by increasing one the other is reduced. This pattern was also observed for the AD digestion of water hyacinth [36], while other reports have suggested that BC improves AD, especially under stressful conditions, such as low ISRs [14].

### 3.2. Biochar Properties and Their Effect on Anaerobic Digestion

#### 3.2.1. Feedstocks Used for Producing the Biochar Added to Anaerobic Digestion

From the reports compiled in Tables 1–4, BC addition enhanced the BMP and  $\mu_m$  by 57% and 83% of the cases, respectively. The greatest improvements of BMP corresponded to slow pyrolysis BCs: ashe juniper-BC 400 and 600 °C, switchgrass-BC 500 °C and canola meal-BC 700 °C [9], corn stalk-BC 400 °C [35], vineyard pruning-BC 550 °C [28], and oak wood-BC 450 °C [37]. For  $\mu_m$ , the BCs whose effect was more favourable were vineyard pruning-BC 550 °C [28], fruitwoods 800 and 900 °C [26,29], corn stalk-BC 400 °C [35], bamboo-BC and pine wood-BC 500 °C [25], and oak wood-BC and water hyacinth-BC 450 °C [10]. Conversely, rice straw-BC has proven repeatedly not to offer a positive impact on AD in comparison to the control [15,16,25]. Generally, woody-derived BCs exhibited the greatest benefits during the AD amendment.

#### 3.2.2. Pyrolysis Temperature

The distribution for the effect of PT for producing the BCs added to AD obtained from the dataset was standardised into box plots (Figure 3). PT exhibited a significant effect on  $\mu_m$  ( $p < 0.05$ ), improving  $\mu_m$  in most cases, with a few exceptions in the literature [10,16,26,30,36–38]. No significant correlation was observed for the PT used for producing the BCs over their effect on BMP or  $\lambda$  ( $p > 0.05$ ). The summary of all reports showed an average improvement of BMP (25%) and  $\mu_m$  (38%) by adding BC. Particularly for slow pyrolysis BCs produced at 400–550 °C the improvement was more significant up to 100%, 400% and 180% for BMP,  $\mu_m$  and  $\lambda$  reduction, respectively [28,31,35], whereas the addition of highly carbonised and aromatic BCs produced at high PT or long pyrolysis retention times generally exhibited a negative effect on AD [16,30,38], with some exceptions.

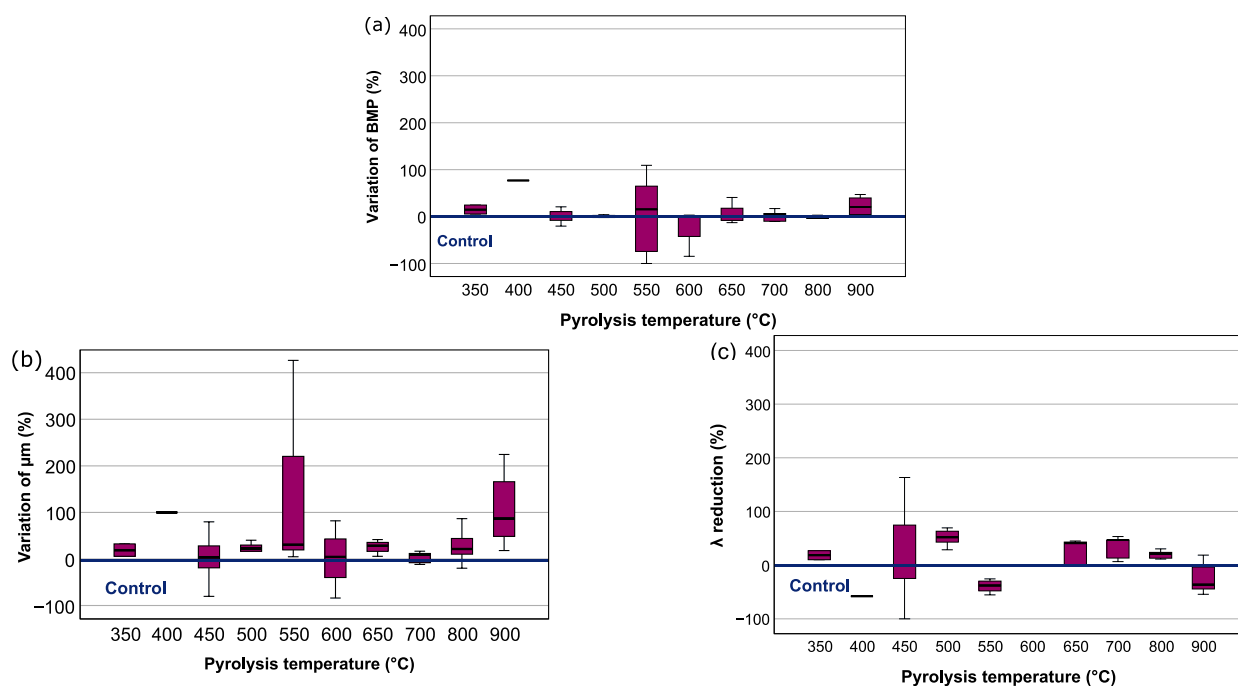


**Figure 3.** Box plot for the distribution of the effect of pyrolysis temperature used for producing the biochar added to anaerobic digestion, described by the relationship with BMP (a);  $\mu_m$  (b), and  $\lambda$  reduction (c).

Temperature is the most important parameter in pyrolysis since it determines most of the properties of the produced BCs, and in consequence, the effect of BC in AD as observed in the PCA (Figure 2) [43]. The initial steps of pyrolysis at 200–400 °C involve the detachment of low-energy bonds, such as acidic hydrogen and oxygen-containing groups (e.g., carboxyl, hydroxyl and formyl groups). It is until 500 °C that the alkyl C structure is further destroyed, resulting in a more aromatic BC [3]. As pyrolysis temperature continues to raise, the graphitisation degree of the BCs increases due to the dehydrogenation and deoxygenation reactions and consequently generation of stable condensed ring compounds [44]. Thus, BCs produced below 500 °C often exhibit a large content of OFGs and volatile matter, while the rise in temperature leads to BCs with lower H and O content, enhanced aromaticity, aromatic ring condensation and a more basic nature [45]. The latter is of importance given that PT is key for the presence of diverse functional groups, including hydroxyl, ketone, aldehyde, amino, ester, nitro, carboxylic, particularly OFGs such as quinone/hydroquinone [10]. Other favourable features of these BCs are electron exchange capacity, and a well-developed surface area and porosity [6]. As PT increases, so do the pH, ash content, and hydrophobicity since more polar functional groups are removed and aromaticity is enhanced [46]. The heterogeneous surface of the BCs donates the BC the ability to interact with the environment and promote DIET reactions between the microorganisms involved in AD. In summary, BCs produced at intermediate temperatures (450–550 °C) could be more adequate for AD than higher temperature ones because they exhibit an extensive redox buffering capacity dominated by OFGs.

### 3.2.3. Biochar Composition

BCs with an ash content of 3.1–6.3%, mainly woody-BCs, generally improved BMP and  $\mu_m$  by 58 and 60% (Figure 4a,b). BCs with ash contents of 6.3–7.8% were generally favourable for reducing  $\lambda$  by an average of 37%, while the oak wood-BC 450 °C with an ash content of 11.7% exhibited an opposite response (Figure 4c). The larger distribution linked to BC with higher ash contents (>11.7%) was restricted to two publications that increased the  $\mu_m$  by four times [10,28]. By increasing PT, the ash content concentrates due to the loss of organic matter [44]. The inorganics within the BCs could provide a source of alkalinity,

conductivity and trace nutrients since Cl, Ca and K could increase the BC conductivity and subsequently improve DIET interactions [47]. Nonetheless, the effect of BC ash content had no significant effect on either BMP,  $\mu_m$  or  $\lambda$  ( $p > 0.05$ ) (Figure 4a–c).

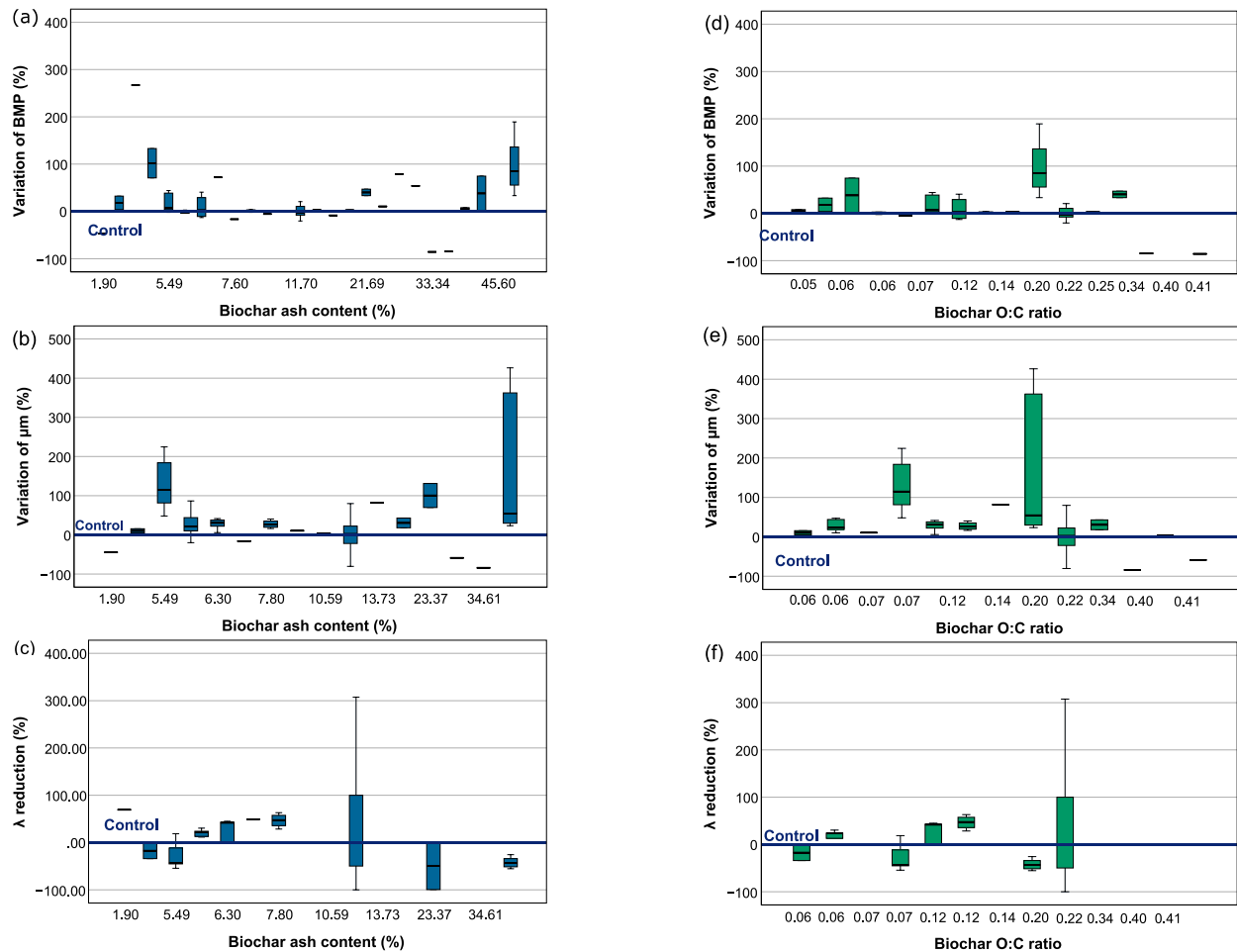


**Figure 4.** Box plot for the distribution of the relation between the variables for the composition of the biochars and their effect in anaerobic digestion parameters: effect of BC ash content on BMP (a),  $\mu_m$  (b) and  $\lambda$  reduction (c); effect of BC O:C ratio on BMP (d),  $\mu_m$  (e), and  $\lambda$  reduction (f).

The BCs used in these reports showed an O:C ratio within a range of 0.06–0.41 (Figure 4d–f). The O:C ratio of the BCs had a significant effect on  $\mu_m$  ( $p < 0.05$ ), while not on BMP or  $\lambda$  reduction. The BCs with an O:C ratio of 0.20 corresponding to BCs produced at 450–500 °C were responsible for increasing the BMP and  $\mu_m$ , by up to two and four times. There is a direct response to PT regarding compounds containing carbon and oxygen. Biomass hydrolysis starts at temperatures as low as 150 °C, reducing thus the content of OH and CH<sub>3</sub>. At 300–400 °C, further loss of O and H is observed as BC is partially carbonised. Pyrolysis requires higher temperatures (up to 500 °C) to drastically reduce these compounds, and increase the content of C=C, due to the transformation of aliphatic compounds into aromatic structures. At 550 °C, the ratio of H:C and O:C decreases even more due to increased aromaticity, while at a higher temperature, the BC is mainly carbonised [48]. Therefore, BC with a moderate level of aromaticity and abundance of OFGs would likely stimulate DIET interactions and improve methane generation as stated above [10,49].

### 3.3. Anaerobic Digestion Conditions

#### 3.3.1. Substrate

The data extracted from the publications have been divided based on the feedstock employed as substrate in AD. The addition of BCs generally improved the AD of model carbohydrate substrates, such as cellulose, glucose and sucrose (Table 1), food waste (Table 2), and the AcoD of citrus peel waste and anaerobic sludge (Table 4). Although that was not the case for the organic fraction of municipal solid waste (OFMSW) [16] (Table 2), and other complex substrates, such as aquatic macrophyte water hyacinth [36] and the seaweed *L. digitata* [38] (Table 4). The more dramatic positive benefits of BC addition were observed for the digestion of complex substrates rich in oil or protein, including sewage sludge, animal manure, bio-oil aqueous phase (BOAP), aqueous pyrolysis liquid (APL) (Table 3), and increasing concentrations of TAN (Table 1). This is highly relevant since the microorganisms involved in AD often struggle to digest substrates rich in lipids or protein, and are affected by ammonia toxicity. Thus, BC augmentation could be particularly useful due to the potential role of BC in facilitating the degradation of such substrates, the rapid consumption of intermediary organic acids [12], and the capacity to adsorb ammonia [50].

#### 3.3.2. Inoculum to Substrate Ratio

The ISR significantly affected BMP yield ( $p < 0.05$ ), but not  $\mu_m$  or  $\lambda$  reduction during AD augmented with BC. The BMP was not affected by BC addition at  $ISR \leq 0.3$ , while it increased up to 80% at  $ISR 0.5-0.9$  (Figure 5a) and was reduced down 50% at an  $ISR 1-2$ . There was no evident trend for the effect of ISR in  $\mu_m$ , which was favoured by 20–50% at variable ISRs, and in some cases increased up to 80–100%, particularly at  $ISR 1-2$  (Figure 5b). BC addition exhibited the most positive effect in reducing  $\lambda$  by 100% at  $ISR 0.5$  (Figure 5c). In summary, BC addition offered a significant and positive effect on BMP at ISRs down to 0.5, which is considered an unfavourable and stressful condition. Although not statistically significant, BC addition improved  $\mu_m$  and  $\lambda$  at most ISR.

Extremely low ISRs are responsible for inclining the microbial population towards the proliferation of acidogens and acetogens, affecting thus methane production [51]. Conversely, large ISRs provide the inoculum with adequate conditions that reduce the  $\lambda$  and the necessity of additives. Thereby the negative correlation between ISR and BCL observed in the PCA (Figure 2) indicates that at a more favourable ISR, less BC is necessary. Therefore, the improvement of AD performance due to BC addition supports the ameliorating benefits of BC and its possible role in facilitating the synergistic interaction between microorganisms, especially at unfavourable conditions, such as low ISR, an observation that has been previously reported [14,29,37].

#### 3.3.3. Biochar Load

The BCL used in the AD reports ranged between 0.03% and 8.0% ( $w/v$ ), with a predominance of 1% (Figure 5d–f). Most BC loads improved or had little effect on the BMP (Figure 5d) and  $\lambda$  reduction (Figure 5f) while increasing BC loads favoured  $\mu_m$  (Figure 5e) although non-statistically significant ( $p > 0.05$ ) for any parameter. Nonetheless, the largest variability was obtained for BC loads of 0.5%, 1.0% and 3%. The AD of cellulose and its co-digestion with *C. vulgaris* at ISRs 0.5–0.9 were promoted at a BCL of 3%, whereas lower BCL was more favourable at ISRs 1–2 [37]. Conversely, the increasing BCL of vineyard pruning-BC 550 °C improved the AD of citrus peel waste [28]. The addition of sawdust BC 500 °C at a BCL of 0.2–1.5% had little effect on the BMP, although it enhanced  $\mu_m$  by 16–40%, exhibiting an optimal BCL of 0.6% [13]. The BCL was highly relevant for high-temperature BCs, as shown by the PCA (Figure 2) where the orthogonality between these two variables suggests that by increasing the PT, the BCL must be reduced. Accordingly, 0.4% of walnut shell-BC 900 °C improved AD, while higher doses (>0.7%) were inhibitory [19]. In summary, low BC loads (~0.4–0.6%) were optimal for improving AD performance, particularly  $\mu_m$ , while higher doses could even be inhibitory.

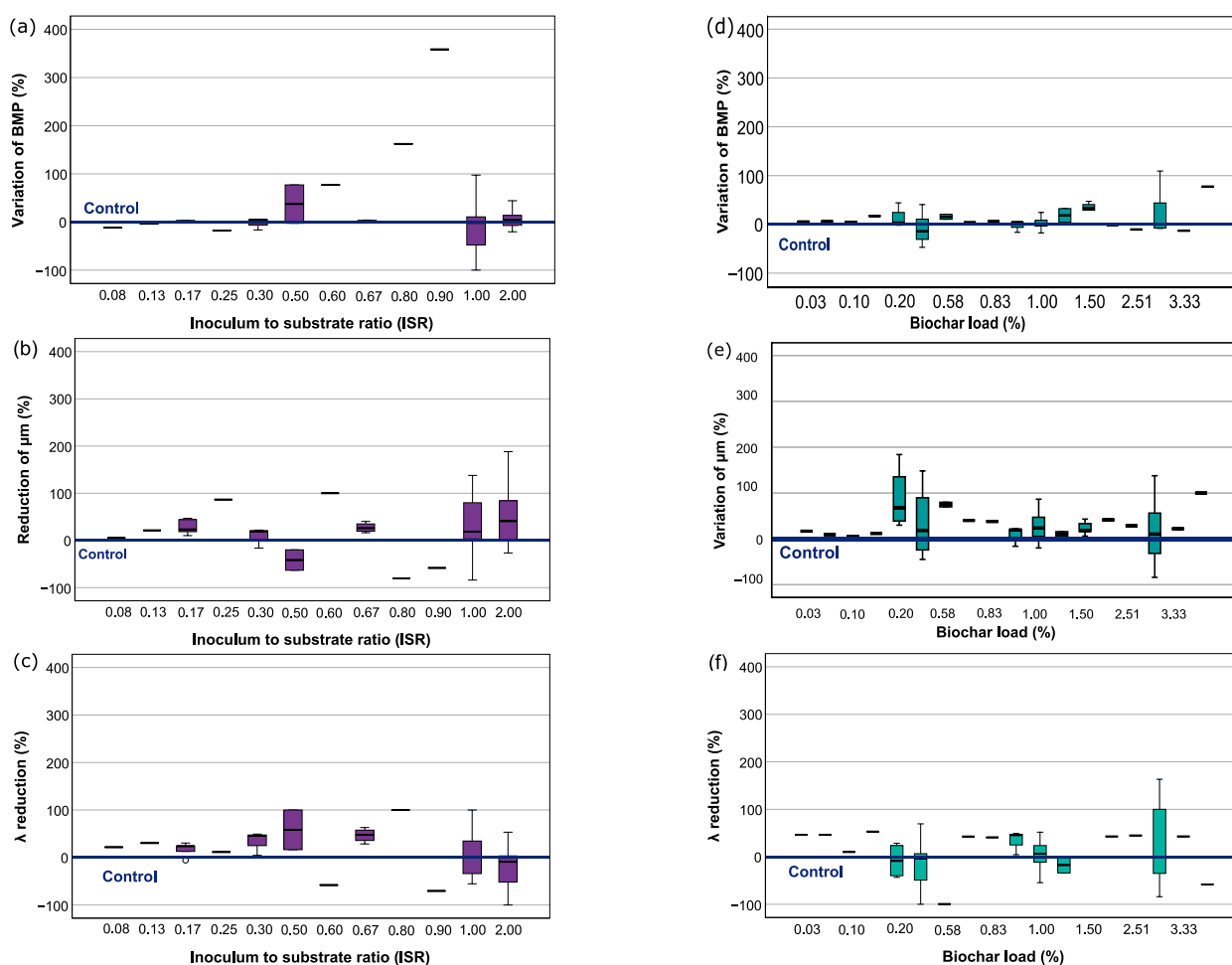


**Figure 5.** Box plot for the distribution of the relation between the variables for digestion conditions composition and their effect in anaerobic digestion parameters: Effect of inoculum to substrate ratio (ISR) on BMP (a),  $\mu_m$  (b) and  $\lambda$  reduction (c); effect of biochar load (BCL) on BMP (d),  $\mu_m$  (e), and  $\lambda$  reduction (f).

### 3.3.4. pH and Buffering Capacity

BC is reported to stabilise AD reactors by raising the pH and promoting methanogenesis even at harmfully high concentrations of VFAs [11,52]. Several reports have evaluated BC addition on AD without performing pH adjustment, and even so, the pH was maintained near neutrality or slightly alkaline [10,16,19,25,31,33,34,36–39,53]. Other studies adjusted the initial pH within the range of 6.8–8.0 [9,12,13,26,27,29,30,32]. The potential of BC to act as a buffering agent has been reported repeatedly [13,34,35,53,54], while others have observed no significant effect [26,38]. Outstanding buffering capacity has been reported for sawdust-BC 500 °C during the AcoD of food waste and dewatered activated sludge [13] and for oak wood-BC 450 °C during the AcoD of *C. vulgaris* and cellulose at ISRs 0.5–0.9 [37].

The buffering capacity of BC is derived predominantly from the organic functional groups [11] and to a lesser extent carbonates and inorganic alkalis (e.g., oxides, hydroxides, sulphates, sulphides, phosphates) [55]. Fundamentally, the role of BC in stabilising the pH of the digester is attributed to an enhanced electron transfer capacity for directing VFA conversion by methanogens involved in DIET. Hence, the redox properties of the BCs are due principally to their organic electron-accepting and donating moieties [6]. The ash content, particularly alkali and alkaline earth metals (e.g., K, Na, Mg and Ca) could influence the alkalinity and conductivity of the BC, and contribute to the catalytic and



buffering capacity [8,46]. Metals contained in the BC, such as Fe, are reported to act as reducing agents and stimulate the degradation of VFAs [27].

#### 4. Conclusions

There is an increasing interest in biochar augmentation to improve anaerobic digestion. However, the operation conditions and outcomes published in the literature often differ, providing ambiguous and even contradictory results. From this compilation, BC addition improved BMP and  $\mu_m$  in 57% and 83% of the conditions tested, which supports the necessity to standardise its application. This work has proven the usefulness of collecting a large dataset from publications and evaluating it under the same scope. PCA stated that the benefits of BC are subjected to the conditions used during pyrolysis that donate the BC with its inherent properties and the AD operating conditions. Of all the BCs used for the experiments in the gathered literature, woody-derived BCs produced by slow pyrolysis at 450–550 °C with an ash content of 3.1–6.3%, and O:C ratio of 0.20 were responsible for having the greatest positive impact in AD by increasing the BMP and  $\mu_m$ , by two and four times the control. The amount of BC added to the digester also influenced the results, as moderate BCL (~0.4–0.6%) could substantially improve AD performance, particularly the production rate, while higher BCL could even be detrimental. The greatest benefit of BC addition was the enhancement of the methane production rate, which could be related to the ability of the BC to interact with its surroundings through its functional groups while promoting DIET synergy. This benefit was more considerable under sub-optimal conditions, such as low ISRs, mono and co-digestion of complex substrates, particularly those rich in lipids and protein where BC augmentation could highlight its potential.

**Supplementary Materials:** The following information can be downloaded at: <https://www.mdpi.com/article/10.3390/en16062523/s1>, Table S1: Data used for the principal component analysis for the effect of biochar addition in methane generation during anaerobic digestion; Table S2: Summarised values for the standardisation of the data used for the principal component analysis. Reference [56] is cited in the supplementary materials.

**Author Contributions:** Conceptualization, J.Q.-N. and A.B.R.; methodology, J.Q.-N.; software, J.Q.-N.; validation, J.Q.-N. and A.B.R.; formal analysis, J.Q.-N.; investigation, J.Q.-N.; resources, J.Q.-N., A.B.R., A.J.B. and L.A.F.; data curation, J.Q.-N.; writing—original draft preparation, J.Q.-N.; writing—review and editing, J.Q.-N. and A.B.R.; visualization, J.Q.-N. and A.B.R.; supervision, A.B.R., A.J.B. and L.A.F.; project administration, A.B.R. and A.J.B.; funding acquisition, J.Q.-N., A.B.R., A.J.B. and L.A.F. All authors have read and agreed to the published version of the manuscript.

**Funding:** This research was funded by the National Council on Science and Technology and the Mexican Secretariat of Energy (CONACYT-SENER), the Autonomous University of Sinaloa, the Biotechnology and Biological Sciences Research Council (BBSRC) and Global Challenges Research Fund (GCRF) through the project BEFWAM Bioenergy, Fertilisers, and clean Water from invasive Aquatic Macrophytes [grant BB/S011439/1].

**Data Availability Statement:** Not applicable.

**Conflicts of Interest:** The authors declare no conflict of interest.

#### Abbreviations

AcoD	Anaerobic co-digestion
AD	Anaerobic digestion
APL	Aqueous pyrolysis liquid
BC	Biochar
BCL	Biochar load
BMP	Biochemical methane potential
BOAP	Bio-oil aqueous phase
CEC	Cation exchange capacity
COD	Carbon oxygen demand



DIET	Direct interspecies electron transfer
EC	Electrical conductivity
FC	Fixed carbon
FDH	Formate dehydrogenases
FW	Food waste
HR	Heating rate
HRT	Hydraulic retention time
ISR	Inoculum to substrate ratio
KMO	Kaiser-Meyer-Olkin method
NR	Not reported
OFG	Oxygenated functional groups
OFMSW	Organic fraction of the municipal solid waste
PC	Principal component
PCA	Principal component analysis
PS	Particle size
PT	Pyrolysis temperature
PV	Pore volume
SA	Surface area
SP	Slow pyrolysis
SS	Sewage sludge
SW	Softwood
TAN	Total ammonia nitrogen
TC	Total carbon
TS	Total solids
VFA	Volatile fatty acids
VM	Volatile matter
VS	Volatile solids
$\mu_m$	Methane production rate
$\lambda$	Lag phase

## References

- Pan, J.; Ma, J.; Zhai, L.; Luo, T.; Mei, Z.; Liu, H. Achievements of Biochar Application for Enhanced Anaerobic Digestion: A Review. *Bioresour. Technol.* **2019**, *292*, 122058. [[CrossRef](#)]
- Wu, Y.; Wang, S.; Liang, D.; Li, N. Conductive Materials in Anaerobic Digestion: From Mechanism to Application. *Bioresour. Technol.* **2020**, *298*, 122403. [[CrossRef](#)]
- Liu, W.-J.; Jiang, H.; Yu, H.-Q. Development of Biochar-Based Functional Materials: Toward a Sustainable Platform Carbon Material. *Chem. Rev.* **2015**, *115*, 12251–12285. [[CrossRef](#)] [[PubMed](#)]
- Zhao, Z.; Zhang, Y.; Woodard, T.L.; Nevin, K.P.; Lovley, D.R. Enhancing Syntrophic Metabolism in Up-Flow Anaerobic Sludge Blanket Reactors with Conductive Carbon Materials. *Bioresour. Technol.* **2015**, *191*, 140–145. [[CrossRef](#)] [[PubMed](#)]
- Zhang, J.; Zhang, F.; Yang, H.; Huang, X.; Liu, H.; Zhang, J.; Guo, S. Graphene Oxide as a Matrix for Enzyme Immobilization. *Langmuir* **2010**, *26*, 6083–6085. [[CrossRef](#)]
- Klöpffel, L.; Keiluweit, M.; Kleber, M.; Sander, M. Redox Properties of Plant Biomass-Derived Black Carbon (Biochar). *Environ. Sci. Technol.* **2014**, *48*, 5601–5611. [[CrossRef](#)] [[PubMed](#)]
- Cruz Viggli, C.; Simonetti, S.; Palma, E.; Pagliaccia, P.; Braguglia, C.; Fazi, S.; Baronti, S.; Navarra, M.A.; Pettiti, I.; Koch, C.; et al. Enhancing Methane Production from Food Waste Fermentate Using Biochar: The Added Value of Electrochemical Testing in Pre-Selecting the Most Effective Type of Biochar. *Biotechnol. Biofuels* **2017**, *10*, 303. [[CrossRef](#)]
- Zhang, J.; Zhao, W.; Zhang, H.; Wang, Z.; Fan, C.; Zang, L. Recent Achievements in Enhancing Anaerobic Digestion with Carbon-Based Functional Materials. *Bioresour. Technol.* **2018**, *266*, 555–567. [[CrossRef](#)] [[PubMed](#)]
- Shanmugam, S.R.; Adhikari, S.; Nam, H.; Kar Sajib, S. Effect of Bio-Char on Methane Generation from Glucose and Aqueous Phase of Algae Liquefaction Using Mixed Anaerobic Cultures. *Biomass Bioenergy* **2018**, *108*, 479–486. [[CrossRef](#)]
- Quintana-Najera, J.; Blacker, A.J.; Fletcher, L.A.; Ross, A.B. The Effect of Augmentation of Biochar and Hydrochar in Anaerobic Digestion of a Model Substrate. *Bioresour. Technol.* **2021**, *321*, 124494. [[CrossRef](#)]
- Wang, G.; Li, Y.; Sheng, L.; Xing, Y.; Liu, G.; Yao, G.; Ngo, H.H.; Li, Q.; Wang, X.C.; Li, Y.Y.; et al. A Review on Facilitating Bio-Wastes Degradation and Energy Recovery Efficiencies in Anaerobic Digestion Systems with Biochar Amendment. *Bioresour. Technol.* **2020**, *314*, 123777. [[CrossRef](#)]
- Lü, F.; Luo, C.; Shao, L.; He, P. Biochar Alleviates Combined Stress of Ammonium and Acids by Firstly Enriching Methanosaeta and Then Methanosarcina. *Water Res.* **2016**, *90*, 34–43. [[CrossRef](#)] [[PubMed](#)]

13. Wang, G.; Li, Q.; Gao, X.; Wang, X.C. Synergetic Promotion of Syntrophic Methane Production from Anaerobic Digestion of Complex Organic Wastes by Biochar: Performance and Associated Mechanisms. *Bioresour. Technol.* **2018**, *250*, 812–820. [[CrossRef](#)] [[PubMed](#)]
14. Shao, L.; Li, S.; Cai, J.; He, P.; Lü, F. Ability of Biochar to Facilitate Anaerobic Digestion Is Restricted to Stressed Surroundings. *J. Clean. Prod.* **2019**, *238*, 117959. [[CrossRef](#)]
15. Wang, C.; Liu, Y.; Gao, X.; Chen, H.; Xu, X.; Zhu, L. Role of Biochar in the Granulation of Anaerobic Sludge and Improvement of Electron Transfer Characteristics. *Bioresour. Technol.* **2018**, *268*, 28–35. [[CrossRef](#)] [[PubMed](#)]
16. Qin, Y.; Wang, H.; Li, X.; Cheng, J.J.; Wu, W. Improving Methane Yield from Organic Fraction of Municipal Solid Waste (OFMSW) with Magnetic Rice-Straw Biochar. *Bioresour. Technol.* **2017**, *245*, 1058–1066. [[CrossRef](#)]
17. Fernandes, P.; Cabral, J.M.S. Bioreactors. In *Multiphase Catalytic Reactors*; John Wiley & Sons, Inc.: Hoboken, NJ, USA, 2016; pp. 156–170.
18. De la Rubia, M.A.; Villamil, J.A.; Rodriguez, J.J.; Mohedano, A.F. Effect of Inoculum Source and Initial Concentration on the Anaerobic Digestion of the Liquid Fraction from Hydrothermal Carbonisation of Sewage Sludge. *Renew. Energy* **2018**, *127*, 697–704. [[CrossRef](#)]
19. Linville, J.L.; Shen, Y.; Ignacio-de Leon, P.A.; Schoene, R.P.; Urgun-Demirtas, M. In-Situ Biogas Upgrading during Anaerobic Digestion of Food Waste Amended with Walnut Shell Biochar at Bench Scale. *Waste Manag. Res.* **2017**, *35*, 669–679. [[CrossRef](#)]
20. Sunyoto, N.M.S.; Zhu, M.; Zhang, Z.; Zhang, D. Effect of Biochar Addition on Hydrogen and Methane Production in Two-Phase Anaerobic Digestion of Aqueous Carbohydrates Food Waste. *Bioresour. Technol.* **2016**, *219*, 29–36. [[CrossRef](#)]
21. Bin Khalid, Z.; Siddique, M.N.I.; Nayeem, A.; Adyel, T.M.; Ismail, S. Bin; Ibrahim, M.Z. Biochar Application as Sustainable Precursors for Enhanced Anaerobic Digestion: A Systematic Review. *J. Environ. Chem. Eng.* **2021**, *9*, 105489. [[CrossRef](#)]
22. Chiappero, M.; Norouzi, O.; Hu, M.; Demichelis, F.; Berruti, F.; Di Maria, F.; Mašek, O.; Fiore, S. Review of Biochar Role as Additive in Anaerobic Digestion Processes. *Renew. Sustain. Energy Rev.* **2020**, *131*, 110037. [[CrossRef](#)]
23. Codignole Luz, F.; Cordiner, S.; Manni, A.; Mulone, V.; Rocco, V. Biochar Characteristics and Early Applications in Anaerobic Digestion—a Review. *J. Environ. Chem. Eng.* **2018**, *6*, 2892–2909. [[CrossRef](#)]
24. Chiappero, M.; Cillerai, F.; Berruti, F.; Mašek, O.; Fiore, S. Addition of Different Biochars as Catalysts during the Mesophilic Anaerobic Digestion of Mixed Wastewater Sludge. *Catalysts* **2021**, *11*, 1094. [[CrossRef](#)]
25. Qin, Y.; Yin, X.; Xu, X.; Yan, X.; Bi, F.; Wu, W. Specific Surface Area and Electron Donating Capacity Determine Biochar’s Role in Methane Production during Anaerobic Digestion. *Bioresour. Technol.* **2020**, *303*, 122919. [[CrossRef](#)]
26. Luo, C.; Lü, F.; Shao, L.; He, P. Application of Eco-Compatible Biochar in Anaerobic Digestion to Relieve Acid Stress and Promote the Selective Colonization of Functional Microbes. *Water Res.* **2015**, *68*, 710–718. [[CrossRef](#)] [[PubMed](#)]
27. Sugiarto, Y.; Sunyoto, N.M.S.; Zhu, M.; Jones, I.; Zhang, D. Effect of Biochar Addition on Microbial Community and Methane Production during Anaerobic Digestion of Food Wastes: The Role of Minerals in Biochar. *Bioresour. Technol.* **2021**, *323*, 124585. [[CrossRef](#)]
28. Martínez, E.J.; Rosas, J.G.; Sotres, A.; Moran, A.; Cara, J.; Sánchez, M.E.; Gómez, X. Codigestion of Sludge and Citrus Peel Wastes: Evaluating the Effect of Biochar Addition on Microbial Communities. *Biochem. Eng. J.* **2018**, *137*, 314–325. [[CrossRef](#)]
29. Cai, J.; He, P.; Wang, Y.; Shao, L.; Lü, F. Effects and Optimization of the Use of Biochar in Anaerobic Digestion of Food Wastes. *Waste Manag. Res.* **2016**, *34*, 409–416. [[CrossRef](#)]
30. Fagbohunge, M.O.; Herbert, B.M.J.; Hurst, L.; Li, H.; Usmani, S.Q.; Semple, K.T. Impact of Biochar on the Anaerobic Digestion of Citrus Peel Waste. *Bioresour. Technol.* **2016**, *216*, 142–149. [[CrossRef](#)]
31. Gómez, X.; Meredith, W.; Fernández, C.; Sánchez-García, M.; Díez-Antolínez, R.; Garzón-Santos, J.; Snape, C.E. Evaluating the Effect of Biochar Addition on the Anaerobic Digestion of Swine Manure: Application of Py-GC/MS. *Environ. Sci. Pollut. Res.* **2018**, *25*, 25600–25611. [[CrossRef](#)]
32. Jang, H.M.; Choi, Y.-K.K.; Kan, E. Effects of Dairy Manure-Derived Biochar on Psychrophilic, Mesophilic and Thermophilic Anaerobic Digestions of Dairy Manure. *Bioresour. Technol.* **2018**, *250*, 927–931. [[CrossRef](#)]
33. Shen, Y.; Linville, J.L.; Ignacio-de Leon, P.A.A.; Schoene, R.P.; Urgun-Demirtas, M. Towards a Sustainable Paradigm of Waste-to-Energy Process: Enhanced Anaerobic Digestion of Sludge with Woody Biochar. *J. Clean. Prod.* **2016**, *135*, 1054–1064. [[CrossRef](#)]
34. Shen, Y.; Linville, J.L.; Urgun-Demirtas, M.; Schoene, R.P.; Snyder, S.W. Producing Pipeline-Quality Biomethane via Anaerobic Digestion of Sludge Amended with Corn Stover Biochar with in-Situ CO<sub>2</sub> Removal. *Appl. Energy* **2015**, *158*, 300–309. [[CrossRef](#)]
35. Torri, C.; Fabbri, D. Biochar Enables Anaerobic Digestion of Aqueous Phase from Intermediate Pyrolysis of Biomass. *Bioresour. Technol.* **2014**, *172*, 335–341. [[CrossRef](#)] [[PubMed](#)]
36. Quintana-Najera, J.; Blacker, A.J.; Fletcher, L.A.; Bray, D.G.; Ross, A.B. The Influence of Biochar Augmentation and Digestion Conditions on the Anaerobic Digestion of Water Hyacinth. *Energies* **2022**, *15*, 2524. [[CrossRef](#)]
37. Quintana-Najera, J.; Blacker, A.J.; Fletcher, L.A.; Ross, A.B. Influence of Augmentation of Biochar during Anaerobic Co-Digestion of *Chlorella Vulgaris* and Cellulose. *Bioresour. Technol.* **2022**, *343*, 126086. [[CrossRef](#)]
38. Deng, C.; Lin, R.; Kang, X.; Wu, B.; O’Shea, R.; Murphy, J.D. Improving Gaseous Biofuel Yield from Seaweed through a Cascading Circular Bioenergy System Integrating Anaerobic Digestion and Pyrolysis. *Renew. Sustain. Energy Rev.* **2020**, *128*, 109895. [[CrossRef](#)]
39. Mumme, J.; Srocke, F.; Heeg, K.; Werner, M. Use of Biochars in Anaerobic Digestion. *Bioresour. Technol.* **2014**, *164*, 189–197. [[CrossRef](#)]

40. Swarbrick, B.; Westad, F. An Overview of Chemometrics for the Engineering and Measurement Sciences. In *Handbook of Measurement in Science and Engineering*; John Wiley & Sons, Inc.: Hoboken, NJ, USA, 2016; Volume 3, pp. 2307–2407.
41. Plonsky, L.; Loewen, S.; Gonulal, T. Exploratory Factor Analysis and Principal Components Analysis. In *Advancing Quantitative Methods in Second Language Research*; Routledge: London, UK, 2015; pp. 182–212.
42. Dandikas, V.; Heuwinkel, H.; Lichti, F.; Drewes, J.E.; Koch, K. Correlation between Biogas Yield and Chemical Composition of Grassland Plant Species. *Energy Fuels* **2015**, *29*, 7221–7229. [[CrossRef](#)]
43. Amonette, J.E.; Joseph, S. Characteristics of Biochar: Microchemical Properties. In *Biochar for Environmental Management: Science and Technology*; Routledge: London, UK, 2009; pp. 65–84.
44. Li, D.C.; Jiang, H. The Thermochemical Conversion of Non-Lignocellulosic Biomass to Form Biochar: A Review on Characterizations and Mechanism Elucidation. *Bioresour. Technol.* **2017**, *246*, 57–68. [[CrossRef](#)]
45. Mafu, L.D.; Neomagus, H.W.J.P.; Everson, R.C.; Strydom, C.A.; Carrier, M.; Okolo, G.N.; Bunt, J.R. Chemical and Structural Characterization of Char Development during Lignocellulosic Biomass Pyrolysis. *Bioresour. Technol.* **2017**, *243*, 941–948. [[CrossRef](#)]
46. Weber, K.; Quicker, P. Properties of Biochar. *Fuel* **2018**, *217*, 240–261. [[CrossRef](#)]
47. Chintala, R.; Schumacher, T.E.; Kumar, S.; Malo, D.D.; Rice, J.A.; Bleakley, B.; Chilom, G.; Clay, D.E.; Julson, J.L.; Papiernik, S.K.; et al. Molecular Characterization of Biochars and Their Influence on Microbiological Properties of Soil. *J. Hazard. Mater.* **2014**, *279*, 244–256. [[CrossRef](#)] [[PubMed](#)]
48. Chan, K.Y.; Xu, Z. Biochar: Nutrient Properties and Their Enhancement. In *Biochar for Environmental Management: Science and Technology*; Routledge: London, UK, 2009; pp. 99–116.
49. Deng, C.; Lin, R.; Kang, X.; Wu, B.; Wall, D.M.; Murphy, J.D. What Physicochemical Properties of Biochar Facilitate Interspecies Electron Transfer in Anaerobic Digestion: A Case Study of Digestion of Whiskey by-Products. *Fuel* **2021**, *306*, 121736. [[CrossRef](#)]
50. Takaya, C.A.; Fletcher, L.A.; Singh, S.; Anyikude, K.U.; Ross, A.B. Phosphate and Ammonium Sorption Capacity of Biochar and Hydrochar from Different Wastes. *Chemosphere* **2016**, *145*, 518–527. [[CrossRef](#)] [[PubMed](#)]
51. Moset, V.; Al-zohairi, N.; Møller, H.B. The Impact of Inoculum Source, Inoculum to Substrate Ratio and Sample Preservation on Methane Potential from Different Substrates. *Biomass Bioenergy* **2015**, *83*, 474–482. [[CrossRef](#)]
52. Meng, X.; Yu, D.; Wei, Y.; Zhang, Y.; Zhang, Q.; Wang, Z.; Liu, J.; Wang, Y. Endogenous Ternary PH Buffer System with Ammonia-Carbonates-VFAs in High Solid Anaerobic Digestion of Swine Manure: An Alternative for Alleviating Ammonia Inhibition? *Process Biochem.* **2018**, *69*, 144–152. [[CrossRef](#)]
53. Paritosh, K.; Vivekanand, V. Biochar Enabled Syntrophic Action: Solid State Anaerobic Digestion of Agricultural Stubble for Enhanced Methane Production. *Bioresour. Technol.* **2019**, *289*, 121712. [[CrossRef](#)]
54. Achi, C.G.; Hassanein, A.; Lansing, S. Enhanced Biogas Production of Cassava Wastewater Using Zeolite and Biochar Additives and Manure Co-Digestion. *Energies* **2020**, *13*, 491. [[CrossRef](#)]
55. Fidel, R.B.; Laird, D.A.; Thompson, M.L.; Lawrinenko, M. Characterization and Quantification of Biochar Alkalinity. *Chemosphere* **2017**, *167*, 367–373. [[CrossRef](#)]
56. Wang, G.; Li, Q.; Dzakpasu, M.; Gao, X.; Yuwen, C.; Wang, X.C. Impacts of Different Biochar Types on Hydrogen Production Promotion during Fermentative Co-Digestion of Food Wastes and Dewatered Sewage Sludge. *Waste Manag.* **2018**, *80*, 73–80. [[CrossRef](#)] [[PubMed](#)]

**Disclaimer/Publisher’s Note:** The statements, opinions and data contained in all publications are solely those of the individual author(s) and contributor(s) and not of MDPI and/or the editor(s). MDPI and/or the editor(s) disclaim responsibility for any injury to people or property resulting from any ideas, methods, instructions or products referred to in the content.